Ultrasonic Characterization of Ibidi µ-Slide I Luer Channel Slides for Studies With Ultrasound Contrast Agents

Zangabad, Reza Pakdaman; Li, Hongchen; Kouijzer, Joop J.P.; Langeveld, Simone A.G.; Beekers, Ines; Verweij, Martin; De Jong, Nico; Kooiman, Klazina

DOI
10.1109/TUFFC.2023.3250202

Publication date
2023

Document Version
Final published version

Published in
IEEE Transactions on Ultrasonics, Ferroelectrics, and Frequency Control

Ultrasonic Characterization of Ibidi μ-Slide I Luer Channel Slides for Studies With Ultrasound Contrast Agents

Reza Pakdaman Zangabad, Hongchen Li, *Graduate Student Member, IEEE*, Joop J. P. Kouijzer, Simone A. G. Langeveld, Inés Beekers, Martin Verweij, *Member, IEEE*, Nico de Jong, *Member, IEEE*, and Klazina Kooiman, *Senior Member, IEEE*

***Abstract*—Understanding and controlling the ultrasound contrast agent (UCA)'s response to an applied ultrasound pressure field are crucial when investigating ultrasound imaging sequences and therapeutic applications. The magnitude and frequency of the applied ultrasonic pressure waves affect the oscillatory response of the UCA. Therefore, it is important to have an ultrasound compatible and optically transparent chamber in which the acoustic response of the UCA can be studied. The aim of our study was to determine the in situ ultrasound pressure amplitude in the ibidi μ-slide I Luer channel, an optically transparent chamber suitable for cell culture, including culture under flow, for all microchannel heights (200, 400, 600, and 800 μm). First, the in situ pressure field in the 800-μm high channel was experimentally characterized using Brandaris 128 ultrahigh-speed camera recordings of microbubbles (MBs) and a subsequent iterative processing method, upon insonification at 2 MHz, 45° incident angle, and 50-kPa peak negative pressure (PNP). Control studies in another cell culture chamber, the CLINIcell, were compared with the obtained results. The pressure amplitude was −3.7 dB with respect to the pressure field without the ibidi μ-slide. Second, using finite-element analysis, we determined the in situ pressure amplitude in the ibidi with the 800-μm channel (33.1 kPa), which was comparable to the experimental value (34 kPa). The simulations were extended to the other ibidi channel heights (200, 400, and 600 μm) with either 35° or 45° incident angle, and at 1 and 2 MHz. The predicted in situ ultrasound pressure fields were between −8.7 and −1.1 dB of the incident pressure field depending on the listed configurations of ibidi slides with different channel heights, applied ultrasound frequencies, and incident angles. In conclusion, the determined ultrasound in situ pressures demonstrate the acoustic compatibility of the ibidi μ-slide I Luer for different channel heights, thereby showing its potential for studying the acoustic behavior of UCAs for imaging and therapy.**

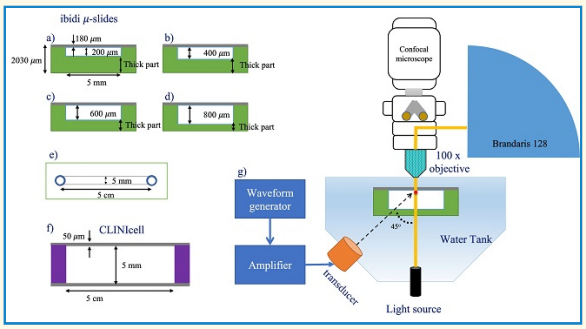

***Index Terms*—Drug delivery, microbubble (MB), ultrahigh-speed imaging, ultrasonic characterization, ultrasound contrast agents (UCAs).**

Manuscript received 10 December 2022; accepted 22 February 2023. Date of publication 27 February 2023; date of current version 26 April 2023. This work was supported by the European Research Council (ERC) through the European Union's Horizon 2020 Research and Innovation Program under Grant 805308. *(Corresponding author: Klazina Kooiman.)*

Reza Pakdaman Zangabad, Hongchen Li, Joop J. P. Kouijzer, Simone A. G. Langeveld, Inés Beekers, and Klazina Kooiman are with the Department of Biomedical Engineering and the Department of Cardiology, Erasmus MC University Medical Center Rotterdam, 3015 GD Rotterdam, The Netherlands (e-mail: rpz3@gatech.edu; k.kooiman@erasmusmc.nl).

Martin Verweij is with the Department of Imaging Physics, Technical University Delft, 2628 CJ Delft, The Netherlands.

Nico de Jong is with the Department of Biomedical Engineering and the Department of Cardiology, Erasmus MC University Medical Center Rotterdam, 3015 GD Rotterdam, The Netherlands, and also with the Department of Imaging Physics, Technical University Delft, 2628 CJ Delft, The Netherlands.

Digital Object Identifier 10.1109/TUFFC.2023.3250202

I. Introduction

ULTRASOUND contrast agents (UCAs) are widely used to enhance the sensitivity and specificity of diagnostic ultrasound imaging in radiology and cardiology [1], [2], [3] and have great potential for local drug delivery [4], [5], [6].

Coated gas microbubbles (MBs) of 1–10 μm in diameter are the most common type of UCA used in diagnostic and therapeutic ultrasound applications [4], [8]. Upon insonification, these MBs compress and expand and, thus, oscillate, which generates a specific acoustic signal that can be used for contrast-enhanced ultrasound imaging [9]. Also, the MB's oscillation behavior can induce bioeffects, such as sonoporation, enhanced endocytosis, and opening of cell–cell contacts [4], [5], [6].

Highlights

- **The in situ ultrasound pressure amplitude in the ibidi μ-slide I Luer channel, an optically transparent chamber suitable for cell culture, including culture under flow, for all micro-channel heights (200, 400, 600, and 800 μm) was determined.**
- **Our findings showed that the in situ pressure varied from -8.7 dB (channel height 400 μm, 2 MHz, 45° angle) to -1.1 dB (channel height 800 μm, 1 MHz, 45° angle). In general, the larger the channel height is, the less the attenuation becomes.**
- **The determined ultrasound in situ pressures demonstrate the potential of the ibidi slide to be used as an ultrasound-compatible device for studying the acoustic behavior of UCAs and ultrasound-mediated drug delivery.**

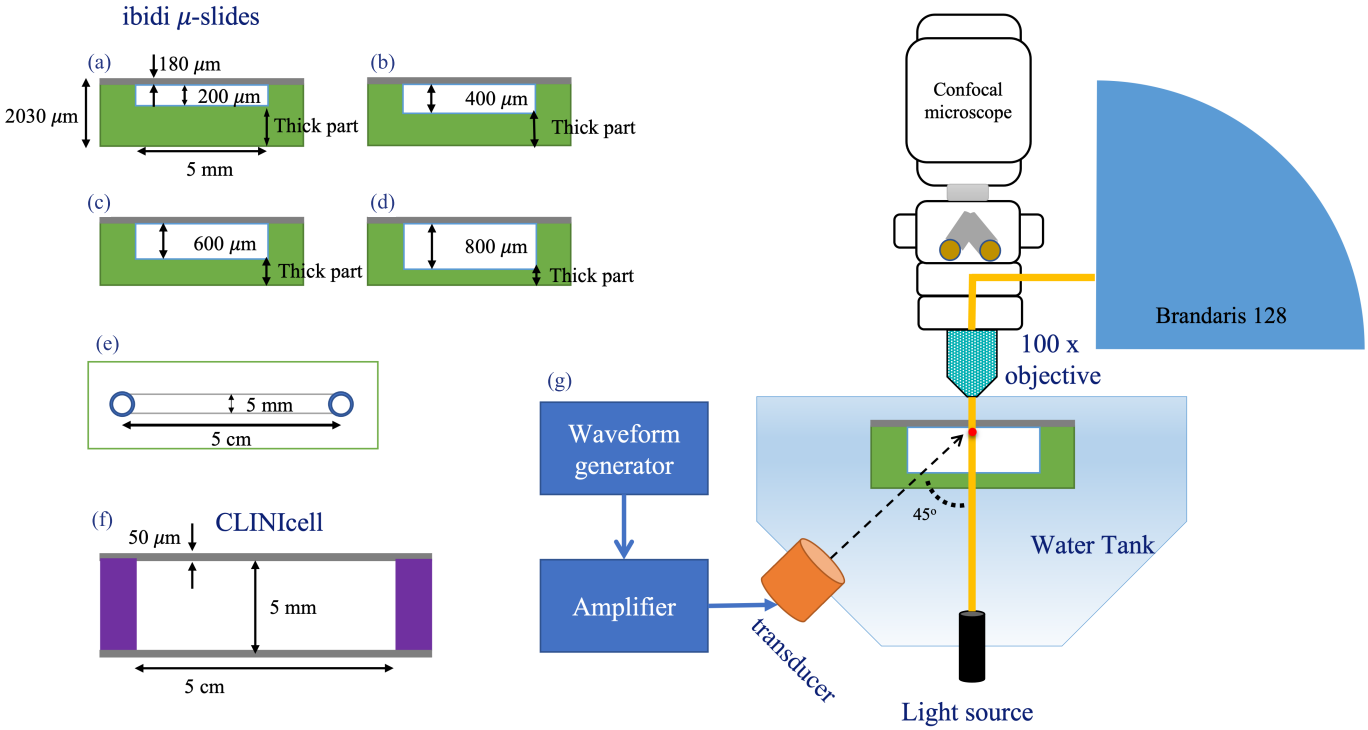

Fig. 1. Schematic view of the experimental setup. (a)–(d) Schematic cross-sectional view of the ibidi slide with different channel heights with the coverslip in gray and the thicker part of the slide in green. (e) Schematic top view of the ibidi slide reproduced and adapted from [7]. (f) Cross-sectional view of the CLINIcell 25 (MABIO) with the 50-μm membrane in gray and the holder in purple. (g) Experimental setup configuration (not drawn to scale).

Currently, the underlying mechanisms for MB-mediated drug delivery are not fully understood [4], [5], [6], which is attributed to the complex interactions among the MB, cell, and drug. These interactions occur at different timescales: in micro-second scale for the MB oscillations, and in millisecond to hour or even days scale for the cellular response and drug uptake [4]. In vitro studies can greatly aid in studying the MB–cell–drug interactions [10]. Recently, several optical in vitro studies have generated more insights into the MB–cell–drug interaction, such as endothelial cell repair upon sonoporation [11], the opening of endothelial cell–cell contacts due to sonoporation [12], involvement of plasma membrane blebbing in reversibly sonoporated cells [13], nanoparticle-loaded MBs being more efficient than coadministration of nanoparticles and MBs for nanoparticle cell delivery [14], and biofilm removal [15]. Only one of these studies [15] included flow, which is an important biological characteristic for mimicking the in vivo situation. The chamber that was used in that study to grow the biofilm under flow was the ibidi μ-slide I Luer (Ibidi GmbH, Gräfelfing, Germany), hereafter referred to as ibidi slide. Previously, the ibidi slide has been used for other studies involving ultrasound, namely, MB-mediated sonoporation [16] and sonoporation and calcium fluctuations [17], [18], estimation and compensation of the attenuation of tissue layers by acoustically observing the MBs [19], development of sonoporation therapy device [20], and evaluation of the photoacoustic effect generated by gold nanorods [21]. Of these studies, only two mentioned the attenuation of the ultrasound by the ibidi slide, namely, less than 2% for the 800-μm channel height slide when insonified through the coverslip using 1.25-MHz ultrasound under a 45° incident angle [18], while this was an attenuation of 19.3% for the 400-μm channel height slide when insonified using 0.5-MHz ultrasound (insonification through which part of the ibidi slide and incident angle not mentioned) [16]. Knowing the in situ pressure is of utmost importance, especially when the cell chamber used may not be acoustically transparent. Without knowing the in situ pressure, treatment effects may not be

fully understood, cannot be correlated with specific outcomes, or translated to the in vivo setting [22]. However, a thorough ultrasonic characterization of the ibidi slide is lacking both experimentally and by modeling. This includes the ultrasonic characterization of all possible ibidi slide channel heights, i.e., 200 and 400 μm as used in [16], 600 and 800 μm as used in [15], [18], [19], and [20] [see Fig. 1(a)–(d)], and insonification directions, as the ultrasound can enter through the coverslip or the thicker part of the ibidi slide, as indicated in Fig. 1(a)–(d). Application of ultrasound through the coverslip is most optimal for inverted microscopes, while application through the thicker part is most optimal for upright microscopes [Fig. 1(g)], as this ensures the smallest optical path and, thus, highest optical resolution for the optically obtained data.

The aim of our study was to quantify the in situ acoustic pressure inside the microchannel of the ibidi slides by two approaches: 1) an experimental investigation using MBs as pressure sensors by recording their oscillation response with the Brandaris 128 ultrahigh-speed camera [23] and 2) a finite-element method (FEM)-based analysis. For 1), MBs inside the ibidi slide with a channel height of 800 μm, i.e., so far the most commonly used channel height for ultrasound studies, were insonified with a low amplitude pressure field of 50-kPa peak negative pressure (PNP) at 2 MHz and under a 45° incident angle. The acoustic pressure experienced by the MBs was derived from their oscillatory response using our previously reported method [24]. For comparison, the same experiments were performed in an acoustically characterized CLINIcell [25]. For 2), the same ultrasound setting as in 1) was validated using FEM. The simulation model was extended to evaluate the pressure field entering through the thicker part of the ibidi slide, for all the ibidi slide channel heights [Fig. 1(a)–(d)], for two sets of insonification angles (35° and 45°), and at the commonly used ultrasound frequencies for drug delivery of 1 and 2 MHz.

II. Materials and Methods

A. MB Preparation

We used self-made MBs in order to compare with previous results of the CLINIcell obtained using the same self-made MBs [24], [25]. The 1,2-distearoyl-sn-glycero-3-phosphocholine (DSPC) was provided by Lipoid GmbH (Ludwigshafen, Germany). The PEG40-stearate was purchased from Sigma-Aldrich (Zwijndrecht, The Netherlands), the 1,2-distearoyl-sn-glycero-3-phosphoethanolamine-N-carboxy-(polyethylene glycol) (DSPE-PEG2000) was purchased from Iris Biotech GmbH (Marktredwitz, Germany), and the 1,2-distearoyl-sn-glycero-3-phosphoethanolamine-N-biotinyl (polyethylene glycol) (DSPE-PEG2000-biotin) was purchased from Avanti Polar Lipids (Alabaster, AL, USA), which are the coating components used in the MBs production. Perfluorobutane (C_4F_{10}) was purchased from F2 Chemicals (Preston, U.K.).

The coating components (84.8-mol% DSPC, 8.2-mol% PEG40-stearate, 5.9-mol% DSPE-PEG2000, and 1.1-mol% DSPE-PEG2000-biotin) were prepared with the indirect method as previously described [26], [27]. Biotinylated lipid-coated MBs with a C_4F_{10} gas core were made using probe sonication at 20 kHz with a sonicator ultrasonic processor XL2020 (HeatSystems, Farmingdale, NY, USA) at power setting 10 for 10 s under C_4F_{10} flow as previously described [26], [27], [28].

To fluorescently label the MBs lipid coating, the lipid dye DiD (D282; Thermo Fisher Scientific) was added before probe sonication. The MBs were washed by flotation using C_4F_{10}-saturated phosphate buffered saline (PBS). In brief, 1 mL of MBs stock solution was added to a 3-mL syringe with a one-way tap. Two mL of C_4F_{10}-saturated PBS was added and incubated for 45 min. Subnatant was removed, and the remaining MBs were resuspended in 1 mL of C_4F_{10}-saturated PBS. The MBs size distribution and concentration were determined using a Coulter Counter Multisizer 3 (Beckman Coulter, Mijdrecht, The Netherlands). Particle quantifications with sizes between 1 and 30 μm were performed using a 50-μm aperture tube with a linear spacing between the 256 channels.

B. Experimental Setup

To prevent nonspecific binding of MBs, the ibidi slides and CLINIcells (MABIO, Tourcoing, France) with 50-μm membranes (25 cm^2) were incubated with, respectively, 200-μL or 12-mL PBS containing 2% (w/v) of bovine serum albumin (BSA; A9418-50G; Sigma-Aldrich) at room temperature for 1 h as previously reported [15], [27]. After incubation, the ibidi slide and the CLINIcells were rinsed three times with PBS prior to the experiment.

To study MB response upon ultrasound insonification, either the MB-containing ibidi slide or CLINIcell with an MB concentration of 1×10^5 MBs/mL was inserted into a water tank at room temperature [Fig. 1(g)], i.e., the same configuration as in [15]. The ultrasound pressure field entered the ibidi slide microchannel through the thick part as indicated in Fig. 1(a)–(d). Both platforms were insonified under a 45° angle by a single-element transducer (2.25-MHz center frequency; 3-in focal distance; −6-dB beamwidth of 5 mm at 2 MHz; V305; Panametrics-NDT, Olympus, Waltham, MA, USA). A single ten-cycle sine wave burst was generated using a waveform generator (Tabor 8026, Tabor Electronics, Tel Hanan, Israel) and was amplified by a broadband amplifier (ENI A-500, Electronics and Innovation, Rochester, NY, USA) to generate 50-kPa PNP at the focal point of the transducer measured by a 1-mm-diameter needle hydrophone (Precision Acoustics, Ltd., Dorset, U.K.).

The custom-built Nikon A1R+ confocal microscope (Nikon Instruments, Amsterdam, The Netherlands), which is coupled to the Brandaris 128 ultrahigh-speed camera [29], was used to place the DiD-containing MBs in focus for the Brandaris 128 ultrahigh-speed recording [23].

For every MB studied, two Brandaris-128 recordings were obtained at around 17 million frames/s. The first recording was recorded without applying ultrasound to obtain a MB diameter baseline. After an 80-ms interval, the second recording was acquired in combination with a ten-cycle sine wave burst with a PNP of 50 kPa. A custom-designed image processing software [30] was used to determine the MB's change in radius over time. Then, the relative excursion of the MB was described as follows:

$$x(t) = \frac{R(t)}{R_0} - 1 \tag{1}$$

where (R_0) represents the initial radius. The amplitude (x_0) of the relative excursion was defined as the maximum of the filtered $x(t)$, where the third-order Butterworth bandpass filter with a bandwidth of 500 kHz centered at center frequency $f_T = 2$ MHz was applied. Next, the acoustic pressure experienced by the MBs was determined using the harmonic oscillator model by fitting the x_0 versus R_0 relationship [24], [25]. The model is defined as follows:

$$x_0 = \frac{|P|/\left(4\pi^2 \rho R_0^2\right)}{\sqrt{\left(f_0^2 - f_T^2\right)^2 + \left(\delta f_T f_0\right)^2}} \tag{2}$$

where $\rho = 1000$ kg/m^3 is the water density and f_0 is the eigenfrequency of the MB and is defined as follows:

$$f_0 = \frac{1}{2\pi}\sqrt{\frac{1}{\rho R_0^2}\left[3\gamma P_0 + \frac{2(3\gamma - 1)\sigma_w}{R_0} + \frac{4\chi}{R_0}\right]} \tag{3}$$

where $\gamma = 1.07$ is the ratio of specific heats for C_4F_{10}, $P_0 = 10^5$ Pa is the ambient pressure, $\sigma_w = 0.072$ N/m is the water surface tension, and χ is the MB shell elasticity. The δ in (2) is the damping coefficient, which is defined as follows:

$$\delta = \frac{\omega_0 R_0}{c} + 2 \cdot \frac{4\mu}{R_0^2 \rho \omega_0} + \frac{4\kappa_s}{R_0^3 \rho \omega_0} \tag{4}$$

where $c = 1500$ m/s is the speed of sound in water at room temperature, $\mu = 10^{-3}$ Pa.s is the viscosity of water, and κ_s is the MB shell viscosity. Subsequently, as previously described [24], by fitting the relative excursion (x_0) of the experimental data to the harmonic oscillator model represented in (2) and minimizing the cost function of the nonlinear least-square method, the shell properties of the MBs and their experienced pressure (P) were determined. The 95% confidence interval values were calculated by using the nonlinear regression parameter confidence interval's function "nlparci" in MATLAB (The Mathworks Inc., Natick, MA, USA).

The shell properties of the MBs are pressure-dependent and influence the oscillatory response of them [31], [32], [33], [34]. Therefore, measurements were performed at 50-kPa PNP to keep the intrinsic nonlinear MBs response at a minimum level [34].

C. Finite/Boundary Element Analysis

A 3-D model of the focused V305 single element transducer with a 3-in focal distance was constructed in COMSOL Multiphysics 5.3a (Burlington, MA, USA). The pressure acoustic, boundary element (pabe) method (BEM) was used to simulate the output pressure (50-kPa PNP) at its focal distance. Using the BEM, it is only required to mesh the surfaces next to the modeling domain. This means that there is less need to create large volumetric meshes necessary for the FEM, making the BEM interfaces powerful for modeling the pressure field radiation and scattering from geometries. The pabe interface was coupled to the solid mechanics (SMs) interface, and then, the SM was coupled to the pressure acoustics, frequency domain (acpr) interface (an FEM interface). Both the CLINIcell and the ibidi slides were modeled using the SM interface, and the channel inside them was assumed water-filled and modeled with the acpr interface. By coupling the various interfaces, a hybrid FEM-BEM model was constructed in which the output pressure field of the transducer was modeled using the BEM and coupled to the SM interface, which itself was coupled to the acpr to fully model all the multiphysics domains.

TABLE I
MATERIAL PROPERTIES OF THE IBIDI SLIDE AND THE CLINICELL [35]

	ibidi slide	CLINIcell
Density (kg/m^3)	1020	1200
Poisson's ratio	0.37	0.381
Young's modulus (Pa)	3.1×10^9	2.3×10^9

The ibidi slide with the channel heights of 200, 400, 600, and 800 μm [Fig. 1(a)–(d)] was simulated for insonification through the thicker side, with either 35° or 45° incident angles, and with 1- and 2-MHz insonification frequencies. The ibidi slide has a channel width of 5 mm and a length of 5 cm [Fig. 1(e)]. The CLINIcell, which is a cell culture chamber consisting of two parallel gas permeable polycarbonate membranes (50-μm membrane, 25-cm^2 area), with a separation of 5 mm [Fig. 1(f)] was also simulated with a 45° incident angle, and with 2-MHz insonification frequency. The material properties of the ibidi slide (Cyclo olefin copolymer, personal communication with Ibidi) and the CLINIcell used in this study are listed in Table I, which were chosen from the software material library [35]. According to the manufacturer, the physical properties of the ibidi slide coverslip and the chamber/walls are similar.

III. RESULTS

A. Experiment

Single MBs with initial diameter (D_0) from 1 to 8 μm were insonified in the ibidi slide with 800-μm channel height ($n = 27$) or in the CLINIcell ($n = 33$) with 50-kPa PNP at 2 MHz under a 45° angle and recorded with the Brandaris 128.

Selected frames of a recorded MB oscillation in the ibidi slide and the CLINIcell are shown in Fig. 2. It can be seen from the figure that the relative excursion of the MB in the ibidi slide [Fig. 2(a)] is lower than that in the CLINIcell [Fig. 2(b)] for the same acoustic settings and similar sized MBs with a resting diameter of 5.3 μm.

Fig. 3 depicts the determined x_0 as a function of D_0 (blue dots). Although variations in response between MBs of similar size were observed in the spread of the data points, the overall x_0 in the ibidi slide was lower than that in the CLINIcell. The arrows in Fig. 3 indicate the MBs whose oscillatory behaviors are depicted in Fig. 2.

The acoustic pressure (P) experienced by the MBs and their shell viscosity (κ_s) and elasticity (χ) as obtained by fitting the relative excursion amplitude (x_0) to the harmonic oscillator model (2) with a 95% confidence interval, are summarized in Table II. Using the parameters estimated in each cell culture platform, the predicted relative excursion amplitude of the MBs as a function of the diameter (1–8 μm with a step of 0.1 μm) was calculated using the harmonic oscillator model (2) and depicted in Fig. 2 with a solid red line.

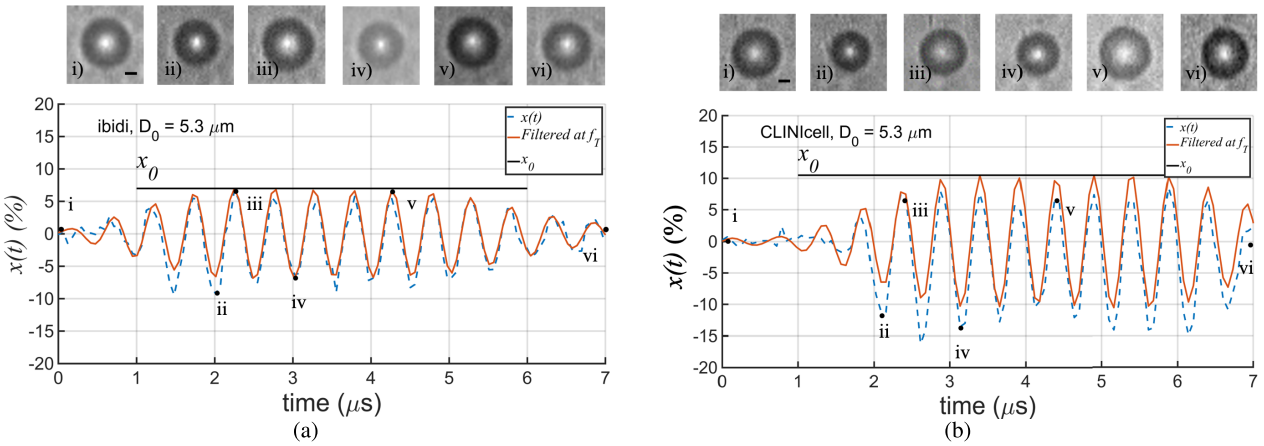

Fig. 2. Selected frames of a Brandaris 128 ultrahigh-speed recording and relative excursion amplitude of a single MB ($D_0 = 5.3$ μm) in (a) 800-μm channel height ibidi slide and (b) CLINIcell, insonified at $f_T = 2$ MHz with 45° angle [1-μm scale bar in frame i) applies to all selected frames ii)–vi)]. Blue dashed line: MB's relative excursion as a function of time [$x(t)$]. Black dots: time points of the selected frames. Red solid line: bandpass filtered $x(t)$ around f_T.

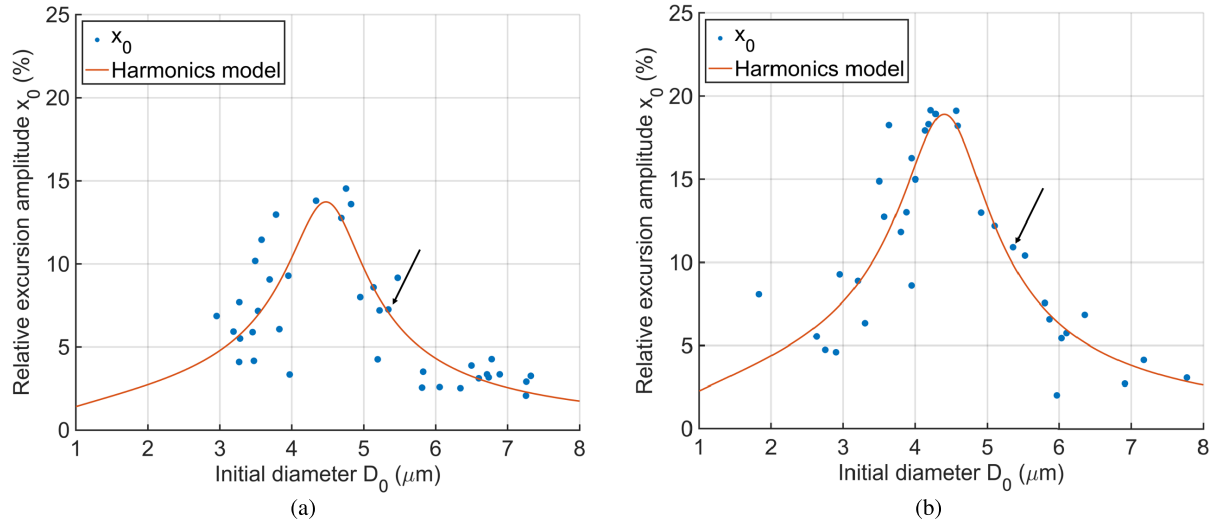

Fig. 3. Relative excursion amplitude (x_0) as a function of initial MB diameter, D_0, in (a) 800-μm channel height ibidi slide and (b) CLINIcell, insonified at $f_T = 2$ MHz with 45° angle. Blue dots: experimentally obtained x_0. Red solid line: corresponding fit using the harmonic oscillator model (2). The arrows show the selected MBs whose relative excursion are depicted in Fig. 2.

TABLE II
MEAN MB SHELL PROPERTIES AND THE EXPERIENCED PRESSURE DERIVED USING THE FIT TO THE HARMONIC OSCILLATOR MODEL WITH THE 95% CONFIDENCE INTERVAL IN PARENTHESES

	Shell viscosity $\times 10^{-9}$ (kg/s)	Shell elasticity (N/m)	PNP (kPa)
ibidi slide	**5.9** (1.1 - 9.7)	**0.17** (0.13 - 0.19)	**34** (27 - 43)
CLINIcell	**5.6** (2.5 - 7.7)	**0.15** (0.12 - 0.18)	**47** (40 - 59)

Normalizing the derived pressure values (P) with respect to the generated pressure at the focus of the transducer in water, 68% and 94% of the pressure coupled into the ibidi slide (through the thick part) and the CLINIcell, respectively. This corresponds to an ultrasound attenuation of −3.3 dB in the ibidi slide and −0.5 dB in the CLINIcell.

B. Finite-Element Analysis

The acoustic pressure was simulated in water, in the ibidi slide, and in the CLINIcell. Fig. 4 shows the simulation results for the ibidi slide with 800-μm channel height, 45° insonification angle at 2 MHz [Fig. 4(a) and (b)]. The result shows that the pressure reaches the maximum of 33.1-kPa PNP at the top of the channel where MBs are recorded and is corresponding to a 66% in situ pressure or −3.6-dB attenuation. Based on the simulation results for the CLINIcell insonified under a 45° angle at 2-MHz frequency [Fig. 4(c) and (d)], 84% of the incident pressure at the membrane coupled into the top membrane corresponding to a −1.4-dB attenuation.

Using the same interface and changing the channel height in the ibidi slide for the different insonification angles and frequencies, the attenuation levels for all the configurations were obtained. Table III shows the summary of the pressure attenuation.

IV. DISCUSSION

The in situ acoustic pressure in the ibidi slide and the CLINIcell was evaluated experimentally using MBs and with FEM-BEM analysis.

For the Brandaris-128 experiments at a 45° insonification angle at 2 MHz, the calculated in situ PNP for the 800-μm height ibidi slide (34 kPa) was lower than that in

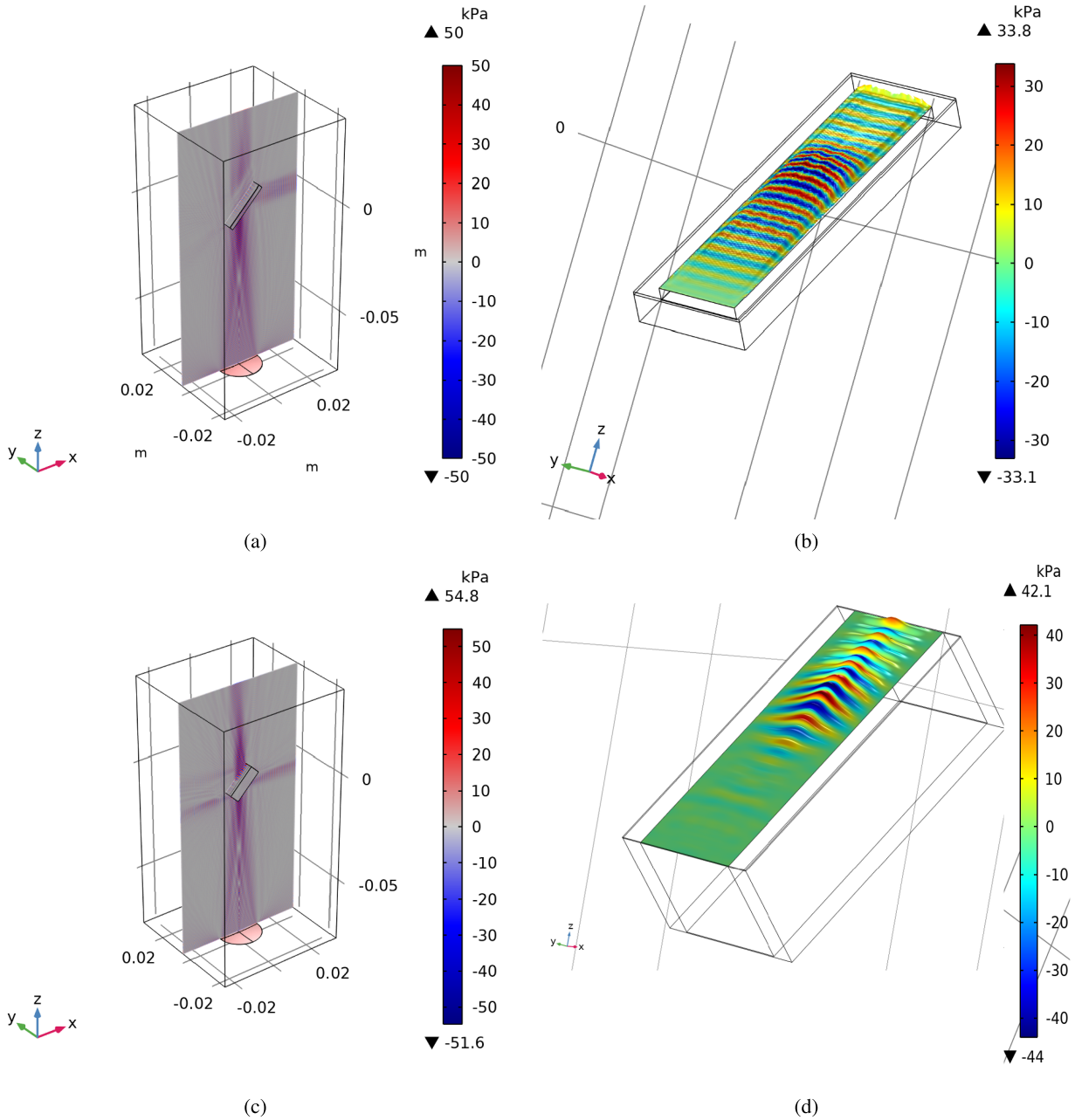

Fig. 4. 3-D simulation results of the BEM-FEM at 2 MHz with 45° insonification angle, in (a) ibidi slide 800-μm channel height and insonified through thicker polymer part; corresponding acoustic pressure at (b), the top of the ibidi channel. 3-D CLINIcell result (c) with corresponding pressure at (d), the top of the CLINIcell membrane.

the CLINIcell (47 kPa). The lower in situ pressure in the ibidi slide was expected, since the ibidi slide is made of cyclo olefin copolymer with a thickness of 1050 μm, while the CLINIcell is made of a polycarbonate gas-permeable film with a membrane thickness of 50 μm. Moreover, the effect of the boundary on MB behavior also needs to be considered [30], [36], [37]. For instance, the frequency of maximum response (f_{MR}) and the amplitude of maximum response (A_{MR}) were previously examined for a subset of MB sizes. For an $R_0 = 2.2$-μm MB insonified at 40 kPa, f_{MR} and A_{MR} decreased by 20% and 50%, respectively, as the MB approached the boundary. However, experimental work on a slightly larger MB $R_0 = 2.3$ μm insonified at 20 kPa revealed an opposite behavior, namely, an increase in f_{MR} by 15% and a decrease in A_{MR} by 60% as the MB approached the boundary [30], [38], [39]. As the membrane stiffness for the ibidi slide and the CLINIcell is different (Table I), this could also contribute to the observed different acoustical response in Fig. 3(a) and (b) for similar sized MBs [40].

The MB's shell elasticity was higher in the ibidi slide (0.17 N/m) than in the CLINIcell (0.15 N/m), while the derived MB's shell viscosity was slightly higher in the ibidi slide (5.9×10^{-9} kg/s) than in the CLINIcell (5.6×10^{-9} kg/s) (Table II). The calculated higher MB shell elasticity for MBs in the ibidi slide in comparison with the CLINIcell is in line with the previously reported shell

elasticity increase with decreasing incident pressure amplitudes [34]. The derived MB shell properties for the MBs in the CLINIcell differed from what was previously reported for the same MB type in the CLINIcell [27]: for the shell viscosity 5.6 (2.5 − 7.7) $\times 10^{-9}$ kg/s (95% confidence interval) in our study versus 9.9 (9.0 − 14.0) $\times 10^{-9}$ kg/s [median (IQR)] in [27] and for the shell elasticity 0.15 (0.12 − 0.18) N/m (95% confidence interval) in our study versus 0.03 (0.01 − 0.06) N/m in [27]. The reasons for this discrepancy could be a difference in acoustic insonification schemes. In our study, the MBs were insonified using one ten-cycle pulse at one frequency, i.e., 2 MHz, while this was 16 eight-cycle pulses at multiple frequencies, i.e., 1–4 MHz in [27]. As a consequence, in our study, we had to use the harmonic oscillator model on the obtained amplitudes for all the MBs, while in [27], the harmonic oscillator model was used on amplitudes of each individual MB over these frequency ranges. In addition, the difference in the range of MB sizes studied (1.8 − 7.8) μm in our study versus (3.5 − 6.5) μm in [27]) could have added to the discrepancy, as the MB shell viscosity is known to increase with increasing diameter [30], [41]. Although both our study and Langeveld et al. [27] applied 50 kPa (PNP) to the MBs and used the same type of calibrated hydrophone to measure the output pressure of the single element transducers, the hydrophone has a 13% uncertainty level. This means that the measured acoustic pressure in the focus of the transducer was 50 ± 6.5 kPa. Therefore, the inverted pressure using the harmonic oscillator model has at least a 13% uncertainty meaning that the in situ pressure can be 13% larger or smaller than the assumed pressure, which also influences the derived MB shell properties.

For the experiments with the Brandaris 128, the commonly used insonification angle of 45° [15], [18], [27], [29] was used. According to the material properties listed in Table I, the longitudinal speed of sound in the ibidi polymer is 2318 m/s and in the CLINIcell membrane is 1899 m/s [42]. Based on the ultrasound refraction theory and Snell's law [42], the critical angle for the ibidi slide is 40.5°. However, since the thickness of the coverslip (180 μm), thicker part of the ibidi slide (1050–1650 μm depending on the channel height), or CLINIcell membrane (50 μm) is smaller than the wavelength at 1 MHz (≈2.3 mm) or 2 MHz (≈1.15 mm), the ultrasound pressure waves will be transmitted through those materials at a 45° insonification angle.

For the ibidi slide with the 800-μm channel height insonified at 2 MHz under a 45° angle, the experimentally obtained in situ acoustic pressure of 34 kPa was comparable to the simulated in situ acoustic pressure of 33.1 kPa. For the CLINIcell insonified under the same conditions, the experimentally obtained in situ pressure also corroborated with the simulation: 47 versus 44 kPa. This corresponded to a 1.4-dB ultrasound attenuation, i.e., 85% of the incident pressure, which is only a 9% difference from the previously reported lower interquartile range value of −2.6 dB, i.e., 74% of the incident angle (IQR −2.6 to 5.0 dB; median −3.8 dB) [25] and is, thus, within the 13% hydrophone uncertainty. Another possible cause for the difference could be the use of the harmonic oscillator model on amplitudes of each individual MB over a 1–4-MHz frequency range in [27] versus amplitudes of all MBs at 2 MHz in our study.

TABLE III
NORMALIZED IN SITU ULTRASOUND PRESSURE ATTENUATION IN THE IBIDI SLIDES OBTAINED FROM FEM-BEM ANALYSIS AT MB RECORDING LOCATION WHERE THE ULTRASOUND INCIDENT PRESSURE FIELD WAS FROM THE THICKER PART OF THE IBIDI SLIDE, UNDER 35° AND 45° INCIDENT ANGLES, AND AT 1- AND 2-MHZ FREQUENCIES

		Ultrasound Attenuation (dB)			
insonified frequency		1 MHz		2 MHz	
incident angle (degree)		35°	45°	35°	45°
ibidi slides channel height (μm)	200	-3.1	-5.5	-7.2	-7.6
	400	-5.0	-2.4	-5.4	-8.7
	600	-4.5	-2.4	-6.8	-7.0
	800	-1.7	-1.1	-4.5	-3.6

Based on the simulation results for the ibidi slide at 1 and 2 MHz for an insonification angle of 35° and 45° (Table III), the in situ pressure varied from −8.7 dB (channel height 400 μm, 2 MHz, 45° angle) to −1.1 dB (channel height 800 μm, 1 MHz, 45° angle). In general, the larger the channel height is, the less the attenuation becomes.

A limitation of the frequency analysis in the simulation is that it is only valid for narrowband waveforms. A rough estimation for narrowband waveforms would be a ten-cycle or more sine waveform with a rectangular window. The Fourier transform of such a waveform is a narrow sinc function that can be approximated as a single delta function at the insonified frequency [43].

V. CONCLUSION

In this study, we have successfully experimentally determined the pressure within the 800-μm channel height ibidi slide, insonified under 45° angle from the bottom of the ibidi slide at 2 MHz. We also successfully simulated the in situ pressure in the ibidi slide for all the channel heights (200, 400, 600, and 800 μm) with a 45° and 35° insonification angle where the 1- and 2-MHz ultrasound pressure waves entered the ibidi slide through the thick polymer part. Controlled MB behavior in the ibidi slide can be achieved when correcting for the determined in situ pressures. Based on the experimental results, the 2-MHz ultrasound in situ pressure was attenuated by 3.7 dB, i.e., 65.5% of the incident pressure, in the ibidi slide with an 800-μm channel height when insonified through the thick polymer part under a 45° angle. The FEM-BEM simulation study corroborated with the experimental study, thereby showing the capability of the simulation to also predict the other configurations. Based on the simulation results, the in situ pressure varied from −8.7 dB (channel height 400 μm, 2 MHz, 45° angle) to −1.1 dB (channel height 800 μm, 1 MHz, 45° angle), thus showing the importance to characterize each configuration. The determined ultrasound in situ pressures demonstrate the potential of the ibidi slide to be used as an ultrasound-compatible device for studying the acoustic behavior of UCAs and ultrasound-mediated drug delivery.

ACKNOWLEDGMENT

The authors would like to thank Robert Beurskens and Frits Mastik from the Department of Biomedical Engineering and

Michiel Manten from the Department of Experimental Medical Instrumentation, Erasmus MC University Medical Center Rotterdam, Rotterdam, The Netherlands, for their technical support.

REFERENCES

[1] J. H. Squires and M. B. McCarville, "Contrast-enhanced ultrasound in children: Implementation and key diagnostic applications," *Amer. J. Roentgenol.*, vol. 217, no. 5, pp. 1217–1231, Nov. 2021.

[2] S. R. Wilson, P. N. Burns, and Y. Kono, "Contrast-enhanced ultrasound of focal liver masses: A success story," *Ultrasound Med. Biol.*, vol. 46, no. 5, pp. 1059–1070, May 2020.

[3] T. R. Porter, S. B. Feinstein, F. J. Ten Cate, and A. E. van den Bosch, "New applications in echocardiography for ultrasound contrast agents in the 21st century," *Ultrasound Med. Biol.*, vol. 46, no. 5, pp. 1071–1081, May 2020.

[4] K. Kooiman et al., "Ultrasound-responsive cavitation nuclei for therapy and drug delivery," *Ultrasound Med. Biol.*, vol. 46, no. 6, pp. 1296–1325, 2020.

[5] S. M. Chowdhury, L. Abou-Elkacem, T. Lee, J. Dahl, and A. M. Lutz, "Ultrasound and microbubble mediated therapeutic delivery: Underlying mechanisms and future outlook," *J. Controlled Release*, vol. 326, pp. 75–90, Oct. 2020.

[6] J. Deprez, G. Lajoinie, Y. Engelen, S. C. De Smedt, and I. Lentacker, "Opening doors with ultrasound and microbubbles: Beating biological barriers to promote drug delivery," *Adv. Drug Del. Rev.*, vol. 172, pp. 9–36, May 2021.

[7] *IBIDI μ-Slide I Luer*. Accessed: Jun. 10, 2021. [Online]. Available: https://ibidi.com/channel-slides/50–slide-i-luer.html

[8] P. Frinking, T. Segers, Y. Luan, and F. Tranquart, "Three decades of ultrasound contrast agents: A review of the past, present and future improvements," *Ultrasound Med. Biol.*, vol. 46, no. 4, pp. 892–908, Apr. 2020.

[9] M. A. Averkiou, M. F. Bruce, J. E. Powers, P. S. Sheeran, and P. N. Burns, "Imaging methods for ultrasound contrast agents," *Ultrasound Med. Biol.*, vol. 46, no. 3, pp. 498–517, Mar. 2020.

[10] G. Lajoinie et al., "In vitro methods to study bubble-cell interactions: Fundamentals and therapeutic applications," *Biomicrofluidics*, vol. 10, no. 1, 2016, Art. no. 011501.

[11] B. Helfield, X. Chen, S. C. Watkins, and F. S. Villanueva, "Transendothelial perforations and the sphere of influence of single-site sonoporation," *Ultrasound Med. Biol.*, vol. 46, no. 7, pp. 1686–1697, Jul. 2020.

[12] I. Beekers et al., "Opening of endothelial cell–cell contacts due to sonoporation," *J. Controlled Release*, vol. 322, pp. 426–438, Jun. 2020.

[13] C. Jia, J. Shi, Y. Yao, T. Han, A. C. H. Yu, and P. Qin, "Plasma membrane blebbing dynamics involved in the reversibly perforated cell by ultrasound-driven microbubbles," *Ultrasound Med. Biol.*, vol. 47, no. 3, pp. 733–750, Mar. 2021.

[14] S. Snipstad, S. Hanstad, A. Bjørkøy, Ý. Mørch, and C. de Lange Davies, "Sonoporation using nanoparticle-loaded microbubbles increases cellular uptake of nanoparticles compared to co-incubation of nanoparticles and microbubbles," *Pharmaceutics*, vol. 13, no. 5, p. 640, Apr. 2021.

[15] J. J. Kouijzer et al., "Vancomycin-decorated microbubbles as a theranostic agent for *Staphylococcus aureus* biofilms," *Int. J. Pharmaceutics*, vol. 609, Nov. 2021, Art. no. 121154.

[16] F. E. Shamout et al., "Enhancement of non-invasive trans-membrane drug delivery using ultrasound and microbubbles during physiologically relevant flow," *Ultrasound Med. Biol.*, vol. 41, no. 9, pp. 2435–2448, 2015.

[17] J.-R. Choi and J. Park, "Investigation of an optical imaging platform integrated with an ultrasound application system for in vitro verification of ultrasound-mediated drug delivery," *Appl. Sci.*, vol. 11, no. 6, p. 2846, Mar. 2021.

[18] J. Park, Z. Fan, and C. X. Deng, "Effects of shear stress cultivation on cell membrane disruption and intracellular calcium concentration in sonoporation of endothelial cells," *J. Biomech.*, vol. 44, no. 1, pp. 164–169, Jan. 2011.

[19] K. Hensel and G. Schmitz, "Method for the estimation and compensation of attenuating tissue layers by the acoustic observation of microbubbles for sonoporation therapy," in *Proc. IEEE Int. Ultrason. Symp.*, Oct. 2010, pp. 1700–1703.

[20] K. Hensel and G. Schmitz, "Performance evaluation of an automatic controlled sonoporation therapy device," in *Proc. IEEE Int. Ultrason. Symp.*, Oct. 2011, pp. 1451–1454.

[21] L. Cavigli et al., "Influence of gold nanorods environment on photoacoustic conversion," in *Proc. Int. Conf. Biophoton. (BioPhotonics)*, May 2015, pp. 1–4.

[22] G. ter Haar et al., "Guidance on reporting ultrasound exposure conditions for bio-effects studies," *Ultrasound Med. Biol.*, vol. 37, no. 2, pp. 177–183, 2011.

[23] C. T. Chin et al., "Brandaris 128: A digital 25 million frames per second camera with 128 highly sensitive frames," *Rev. Sci. Instrum.*, vol. 74, no. 12, pp. 5026–5034, 2003.

[24] I. Beekers et al., "Acoustic characterization of a vessel-on-a-chip microfluidic system for ultrasound-mediated drug delivery," *IEEE Trans. Ultrason., Ferroelectr., Freq. Control*, vol. 65, no. 4, pp. 570–581, Apr. 2018.

[25] I. Beekers, T. van Rooij, A. F. W. van der Steen, N. de Jong, M. D. Verweij, and K. Kooiman, "Acoustic characterization of the CLINIcell for ultrasound contrast agent studies," *IEEE Trans. Ultrason., Ferroelectr., Freq. Control*, vol. 66, no. 1, pp. 244–246, Jan. 2019.

[26] S. A. Langeveld et al., "Ligand distribution and lipid phase behavior in phospholipid-coated microbubbles and monolayers," *Langmuir*, vol. 36, no. 12, pp. 3221–3233, 2020.

[27] S. A. G. Langeveld, I. Beekers, G. Collado-Lara, A. F. W. van der Steen, N. de Jong, and K. Kooiman, "The impact of lipid handling and phase distribution on the acoustic behavior of microbubbles," *Pharmaceutics*, vol. 13, no. 1, p. 119, Jan. 2021.

[28] A. L. Klibanov et al., "Detection of individual microbubbles of ultrasound contrast agents: Imaging of free-floating and targeted bubbles," *Investigative Radiol.*, vol. 39, no. 3, pp. 187–195, 2004.

[29] I. Beekers et al., "Combined confocal microscope and Brandaris 128 ultra-high-speed camera," *Ultrasound Med. Biol.*, vol. 45, no. 9, pp. 2575–2582, 2019.

[30] S. M. Van der Meer et al., "Microbubble spectroscopy of ultrasound contrast agents," *J. Acoust. Soc. Amer.*, vol. 121, no. 1, pp. 648–656, 2007.

[31] B. Helfield, X. Chen, B. Qin, and F. S. Villanueva, "Individual lipid encapsulated microbubble radial oscillations: Effects of fluid viscosity," *J. Acoust. Soc. Amer.*, vol. 139, no. 1, pp. 204–214, Jan. 2016.

[32] C. Tremblay-Darveau et al., "The role of microbubble echo phase lag in multipulse contrast-enhanced ultrasound imaging," *IEEE Trans. Ultrason., Ferroelectr., Freq. Control*, vol. 65, no. 8, pp. 1389–1401, Aug. 2018.

[33] S. Keller, M. Bruce, and M. A. Averkiou, "Ultrasound imaging of microbubble activity during sonoporation pulse sequences," *Ultrasound Med. Biol.*, vol. 45, no. 3, pp. 833–845, Mar. 2019.

[34] Y. Gong, M. Cabodi, and T. M. Porter, "Acoustic investigation of pressure-dependent resonance and shell elasticity of lipid-coated monodisperse microbubbles," *Appl. Phys. Lett.*, vol. 104, no. 7, Feb. 2014, Art. no. 074103.

[35] W. D. Callister, *Materials Science and Engineering: An Introduction; Solutions Manual to Accompany*. Hoboken, NJ, USA: Wiley, 1994.

[36] V. Garbin et al., "Changes in microbubble dynamics near a boundary revealed by combined optical micromanipulation and high-speed imaging," *Appl. Phys. Lett.*, vol. 90, no. 11, 2007, Art. no. 114103.

[37] M. Overvelde et al., "Nonlinear shell behavior of phospholipid-coated microbubbles," *Ultrasound in Med. Biol.*, vol. 36, no. 12, pp. 2080–2092, 2010.

[38] M. Overvelde, V. Garbin, B. Dollet, N. de Jong, D. Lohse, and M. Versluis, "Dynamics of coated microbubbles adherent to a wall," *Ultrasound Med. Biol.*, vol. 37, no. 9, pp. 1500–1508, Sep. 2011.

[39] M. L. J. Overvelde, "Ultrasound contrast agents: Dynamics of coated bubbles," Ph.D. dissertation, Dept. Sci. Technol., Univ. Twente, Enschede, The Netherlands, 2010.

[40] A. A. Doinikov, L. Aired, and A. Bouakaz, "Acoustic scattering from a contrast agent microbubble near an elastic wall of finite thickness," *Phys. Med. Biol.*, vol. 56, no. 21, p. 6951, 2011.

[41] T. van Rooij et al., "Non-linear response and viscoelastic properties of lipid-coated microbubbles: DSPC versus DPPC," *Ultrasound Med. Biol.*, vol. 41, no. 5, pp. 1432–1445, 2015.

[42] G. S. Kino, *Acoustic Waves: Devices, Imaging, and Analog Signal Processing (Prentice-Hall Signal Processing Series)*. Upper Saddle River, NJ, USA: Prentice-Hall, 1987.

[43] A. V. Oppenheim et al., *Signals & Systems*. London, U.K.: Pearson, 1997.